SLAC – PUB – 3761
DESY 85 – 97
August 1985
(E)

Formation of $\delta(980)$ and $A_2(1320)$ in Photon–Photon Collisions*

D. Antreasyan,[i] D. Aschman,[b] D. Besset,[k] J. K. Bienlein,[e] E. D. Bloom,[l] I. Brock,[c] R. Cabenda,[k] A. Cartacci,[g] M. Cavalli-Sforza,[k]‖ R. Clare,[l] G. Conforto,[g] S. Cooper,[l] R. Cowan,[k]‖ D. Coyne,[k]‖ G. Drews,[e] A. Engler,[c] G. Folger,[f] A. Fridman,[l]† J. Gaiser,[l] D. Gelphman,[l]‖ G. Godfrey,[l] F. H. Heimlich,[h] R. Hofstadter,[l] J. Irion,[i] Z. Jakubowski,[d] S. Keh,[m] H. Kilian,[m] I. Kirkbride,[l] T. Kloiber,[e] W. Koch,[e] A. C. König,[j] K. Königsmann,[m] R. W. Kraemer,[c] R. Lee,[l]‖ S. Leffler,[l] R. Lekebusch,[h] P. Lezoch,[h] A. M. Litke,[l]‖ W. Lockman,[l] S. Lowe,[l] B. Lurz,[f] D. Marlow,[c] W. Maschmann,[h] T. Matsui,[l] P. McBride,[i] F. Messing,[c] W. J. Metzger,[j] B. Monteleoni,[g] R. Nernst,[h] C. Newman-Holmes,[k] B. Niczyporuk,[l]‡ G. Nowak,[d] C. Peck,[a] P. G. Pelfer,[g] B. Pollock,[l] F. C. Porter,[a] D. Prindle,[c] P. Ratoff,[a] B. Renger,[c] C. Rippich,[c] M. Scheer,[m] P. Schmitt,[m] M. Schmitz,[e] J. Schotanus,[j] A. Schwarz,[l] D. Sievers,[h] T. Skwarnicki,[e]‡ K. Strauch,[i] U. Strohbusch,[h] J. Tompkins,[l] H.-J. Trost,[e] R. T. Van de Walle,[j] H. Vogel,[c] U. Volland,[f] K. Wachs,[e] K. Wacker,[l] W. Walk,[j] H. Wegener,[f] D. Williams,[i] P. Zschorsch[e]

(THE CRYSTAL BALL COLLABORATION)

[a] *California Institute of Technology, Pasadena, USA*
[b] *University of Cape Town, South Africa*
[c] *Carnegie-Mellon University, Pittsburgh, USA*
[d] *Cracow Institute of Nuclear Physics, Cracow, Poland*
[e] *Deutsches Elektronen Synchrotron DESY, Hamburg, Germany*
[f] *Universität Erlangen-Nürnberg, Erlangen, Germany*
[g] *INFN and University of Firenze, Italy*
[h] *Universität Hamburg, I. Institut für Experimentalphysik, Hamburg, Germany*
[i] *Harvard University, Cambridge, USA*
[j] *University of Nijmegen and NIKHEF-Nijmegen, The Netherlands*
[k] *Princeton University, Princeton, USA*
[l] *Department of Physics, HEPL, and Stanford Linear Accelerator Center, USA*
[m] *Universität Würzburg, Würzburg, Germany*

ABSTRACT. The reaction $\gamma\gamma \to \pi^0\eta$ has been investigated with the Crystal Ball detector at DORIS II. Formation of $\delta(980)$ and $A_2(1320)$ has been observed with $\gamma\gamma$ partial widths $\Gamma_{\gamma\gamma}(A_2) = (1.14 \pm 0.20 \pm 0.26)$ keV and $\Gamma_{\gamma\gamma}(\delta) \times \mathrm{BR}(\delta \to \pi\eta) = (0.19 \pm 0.07\,^{+0.10}_{-0.07})$ keV.

Submitted to *Physical Review D*

* Work supported in part by the Department of Energy under contracts DE-AC03-81ER40050 (CIT), DE-AC02-76ER03066 (CMU), DE-AC02-76ER03064 (Harvard), DE-AC02-76ER03072 (Princeton), DE-AC03-76SF00515 (SLAC), and DE-AS03-76SF00326 (Stanford), and by the National Science Foundation under Grants PHY75-22980 (CIT), PHY84-07870 (HEPL), and PHY82-08761 (Princeton).

‖Present Address: *Institute for Particle Physics, University of California, Santa Cruz, California 95064, USA*
†Permanent Address: *DPHPE, Centre d'Etudes Nucléaires de Saclay, Gif-sur-Yvette, France*
‡Permanent Address: *Cracow Institute of Nuclear Physics, Cracow, Poland*

The χ states observed in the $c\bar{c}$ and $b\bar{b}$ systems have been understood as fine structure triplets of P-wave quark-antiquark states with even charge conjugation. The light $q\bar{q}$ states with the same spin structure, namely the light scalar, pseudovector and tensor mesons, have been more difficult to understand, mainly because states of different flavor are not well separated in mass and are believed to mix with each other. Studying the coupling to two photons offers useful information for the classification of tensor and scalar mesons (pseudovectors do not couple to two real photons). Those tensor mesons which are expected to couple to two photons (f, f', A_2) have been observed in photon-photon collisions and the measured $\gamma\gamma$ partial widths agree well with the naive quark model with approximate ideal mixing. In contrast, there is considerable disagreement about how to classify the known scalar mesons. In particular, there is the question of whether they contain two or four valence quarks (states with no valence quarks, gluonia, may further complicate the question). Scalar mesons have so far not been observed in photon-photon collisions.

In this paper we report on an investigation of the reaction $\gamma\gamma \to \pi^0\eta$ observed in the 4-photon final state with the Crystal Ball at DORIS II. A similar analysis was done by the Crystal Ball at SPEAR[1] in which A_2 formation was observed for the first time. In the present analysis, with ≈ 6 times the statistics, we have made a new measurement of $\Gamma_{\gamma\gamma}(A_2)$ and we have observed and measured for the first time the formation of the scalar meson $\delta(980)$ in $\gamma\gamma$ collisions.

The $\gamma\gamma$ initial state is created by e^+e^- collisions, where each lepton radiates a low q^2 virtual photon. The leptons scatter to a very low or zero angle and are not observed. The $\gamma\gamma$ reaction products are detected and their two-photon origin is identified by the very low total transverse momentum p_T with respect to the beam axis. It is necessary to identify and measure the momenta of all particles in the exclusive final state.

The Crystal Ball detector has been described in detail elsewhere.[2] Briefly, it consists of 672 NaI(Tl) shower counters which detect photons with good spatial and energy resolution. Each shower counter is shaped like a truncated triangular pyramid pointing to the e^+e^- interaction point and is viewed by a phototube. Together they form a hollow sphere of 16 radiation lengths (r.l.) thickness covering 93% of 4π solid angle, with two holes for the beam pipe. An additional 5% of 4π is covered by NaI(Tl) endcaps. Charged particles are detected in a set of cylindrical proportional tube chambers with charge-division read-out. There were originally 3 double-layered chambers filled with Magic Gas, which have gradually been replaced by a new set of 4 double layers filled with an $Ar - CO_2 -$ methane mixture. The beam pipe has a thickness of 0.017 r.l. and each chamber adds 0.010 r.l. in the old and 0.019 r.l. in the new configuration.

The data used for this analysis represent an integrated luminosity $\mathcal{L} = 110\,\mathrm{pb}^{-1}$ and have been taken over a period of two years in the region of the Υ resonances, i.e., at beam energies between 4.7 and 5.3 GeV.

The apparatus is triggered by a number of conditions based on the distribution of energy in the NaI(Tl) crystals. The trigger which has been designed to be efficient for $\gamma\gamma$ reactions requires approximate p_T balance in addition to a total energy above a threshold which has

been set at either 980 or 1170 MeV in different running periods. This threshold is too high for low-mass $\pi^0\eta$ events; we have therefore included other, less efficient triggers with lower thresholds for this analysis. The second trigger requires approximate balance of the total momentum with either a total energy threshold of 770 MeV or a veto on energy in the crystals closest to the beam. The third kind of trigger used in this analysis requires at least 85 MeV each in two groups of 9 crystals which are nearly back-to-back, again with a veto on energy deposited close to the beam.

All events have been passed through a filter program which selects candidate events for $\gamma\gamma$ collisions by requiring $p_T < 200$ MeV and the total energy seen less than 80% of the e^+e^- center-of-mass energy. The total transverse momentum p_T has been calculated by assigning a momentum vector to each crystal with magnitude equal to the energy seen in that crystal. The vectors for all crystals in the ball are summed and the transverse components of the sum are used.

Out of these preselected events, candidate events for the 4-photon final state have been selected by the following criteria:

- ▷ The total energy seen in all endcap crystals must be less than 40 MeV.
- ▷ There must be exactly 4 clusters of energy of at least 20 MeV which are considered as photon candidates.
- ▷ The photons must be within $|\cos\Theta| < 0.9$, where Θ is the angle between a photon and the positron beam.
- ▷ The lateral energy deposition pattern of each photon must be consistent with that expected for an electromagnetic shower.
- ▷ p_T (now calculated from the photon energies and directions) must be less than 100 MeV. (Events failing this cut have been kept to study the p_T-distribution, e.g., for Fig. 2 below).
- ▷ Events have been removed when there were hits in the tube chambers close in ϕ to a photon, where ϕ is the azimuthal direction around the beam axis. (The Θ information has been ignored for this cut because the main background comes from beam-gas interactions which did not necessarily originate at the e^+e^- interaction point.)
- ▷ The trigger requirements have been reproduced in software, with thresholds slightly more restrictive than the electronic thresholds. This cut has been made to be able (a) to calculate the trigger efficiency and (b) to correct for the varying trigger conditions in different running periods.

We then group the four photons of each event into two pairs (there are three ways to do so) and make a scatter plot of the higher versus the lower pair mass $M_{\gamma\gamma}$ (Fig. 1a). There is a strong peak corresponding to $\pi^0\pi^0$ events and a cluster of $\pi^0\eta$ events. Most other entries are wrong combinations from these two types of events. In order to remove background from under the $\pi^0\eta$ signal, we discard events in the $\pi^0\pi^0$ peak, i.e., $100 < M_{\gamma\gamma} < 170$ MeV for both $M_{\gamma\gamma}^{low}$ and $M_{\gamma\gamma}^{high}$ (Fig. 1b).

We have selected $\pi^0\eta$ events by requiring $100 < M_{\gamma\gamma}^{low} < 170$ MeV and $490 < M_{\gamma\gamma}^{high} <$

600 MeV. Non-$\pi^0\eta$ background has been studied using events in the sideband, i.e., events outside the region defined above, but within $65 < M_{\gamma\gamma}^{low} < 205$ MeV and $435 < M_{\gamma\gamma}^{high} < 655$ MeV (the sideband has 3 times the area of the $\pi^0\eta$ region). There are 336 $\pi^0\eta$ and 112 sideband events. These events have then been kinematically fitted using the two mass constraints, and the fit results have been used throughout the remainder of the analysis.

The p_T^2 distribution of the $\pi^0\eta$ events (Fig. 2) shows a peak at zero as expected for a $\gamma\gamma$ reaction. The p_T^2 distribution of sideband events, scaled by the ratio of areas in the mass scatter plot (shaded histogram in Fig. 2), is flat with a small enhancement at zero which is caused by wrong combinations from events with two-photon origin.

The distribution of the effective mass (W) of $\pi^0\eta$ (Fig. 3) shows two peaks, one at the mass of the $\delta(980)$, another at the mass of the $A_2(1320)$. These are the only two resonances with a known $\pi\eta$ decay mode.[3] The scaled W distribution for sideband events (shaded histogram in Fig. 3) shows no such structure.

In order to obtain the cross section for $\gamma\gamma \to \pi^0\eta$, the observed sideband-subtracted event spectrum must be corrected for the detection inefficiency and the W-dependent $\gamma\gamma$ luminosity. The event distribution $d^2N/dW\,d|\cos\Theta^*|$ is related to the cross section for $\gamma\gamma \to \pi^0\eta$ as expressed in the following formula:

$$\frac{d^2N}{dW\,d|\cos\Theta^*|} = \frac{d\sigma_{\gamma\gamma}(W,\cos\Theta^*)}{d|\cos\Theta^*|}\mathcal{L}\int_{\vec{x}} F_{\gamma\gamma}(W,\vec{x})\,E(W,\vec{x},\cos\Theta^*)\,d\vec{x},$$

where Θ^* is the angle between the positron beam and the π^0 in the $\gamma\gamma$ rest frame, $E(W,\vec{x},\cos\Theta^*)$ is the detection efficiency and $\vec{x}$ is a set of variables defining the kinematics of the undetected outgoing e^+ and e^- at given W. $F_{\gamma\gamma}(W,\vec{x})$ is the $\gamma\gamma$ flux (i.e., the ratio of $\gamma\gamma$ luminosity to e^+e^- luminosity) which we have calculated using the formula given by Bonneau, Gourdin and Martin,[4] neglecting terms due to longitudinal photons.

The detection efficiency has been determined by Monte Carlo methods. Events of the type $\gamma\gamma \to \pi^0\eta$ have been generated with a distribution given by the fully differential form of the formula above, but with E set to unity and $d\sigma_{\gamma\gamma}(W,\cos\Theta^*)/d|\cos\Theta^*|$ chosen to uniformly populate the full $\cos\Theta^*$ and W range. These events have then been passed through a detector simulation program based on the shower development code EGS[5] and finally through the same analysis chain as the real events, except for the cut on chamber hits. The generated events have been divided into bins of W and $|\cos\Theta^*|$. Comparing in each bin the number of accepted with the number of generated events results in a two-dimensional acceptance function, the $\gamma\gamma$-flux-weighted average of $E(W,\vec{x},\cos\Theta^*)$ over $\vec{x}$. The average acceptance is 7.5%. Most of the inefficiency is due to events where one or more photons left the ball through the beam-pipe openings.

The efficiency of the cut on chamber hits varies with chamber performance, chamber configuration, and background conditions. It has not been simulated by Monte Carlo, but has been measured separately for each running period using $\gamma\gamma \to \pi^0\pi^0$ events in the $f(1270)$ region. The above cuts, without the cut on chamber hits, yield a sample of ≈ 2000 f events

with negligible background. The average efficiency of the cut on chamber hits is 64%. Most of the rejected f events have a photon converted to an e^+e^- pair in the beam pipe or the chamber material.

The cross section has been calculated by giving each event a weight consisting of the inverse of the product of efficiency and $\gamma\gamma$-luminosity. The efficiency is a luminosity-weighted average including the run-dependent chamber and trigger efficiencies. The cross section is shown in Fig. 4 as function of W for $|\cos\Theta^*| < 0.9$.

The solid curve in Fig. 4 shows the result of a fit with 3 contributions:

- a relativistic spin-0 Breit-Wigner function[6] with mass 983 MeV and width 54 MeV[3] for the δ, folded with a Gaussian with $\sigma = 15$ MeV mass resolution, with $\Gamma_{\gamma\gamma}(\delta)$ as a free parameter;
- a relativistic spin-2 Breit-Wigner function[6] with mass 1318 MeV and width 110 MeV[3] for the A_2, folded with a Gaussian with $\sigma = 23$ MeV mass resolution, with $\Gamma_{\gamma\gamma}(A_2)$ as a free parameter;
- a smooth function with 3 parameters to describe the non-resonant contribution (broken curve).

We have obtained a good fit with $\chi^2 = 20.1$ for 18 degrees of freedom. In a separate fit (with $\chi^2 = 16.3$ for 14 degrees of freedom) the resonance masses and widths have also been free parameters, resulting in $m(\delta) = (1005 \pm 9)$ MeV, $\Gamma(\delta) = (32^{+50}_{-32})$ MeV,[7] $m(A_2) = (1315 \pm 15)$ MeV and $\Gamma(A_2) = (117 \pm 86)$ MeV. The errors are statistical only; there is an additional systematic error of 2% on the masses. We find reasonable agreement with the nominal parameters.

In order to check our assignment of the δ and A_2 resonances to the peaks observed and to be able to extrapolate to the full $\cos\Theta^*$ range, we investigate the decay angular distributions. Fig. 5 shows the differential cross section $d\sigma/d|\cos\Theta^*|$ for the W ranges $900 - 1100$ MeV (containing the δ peak) and $1100 - 1480$ MeV (containing the A_2 peak). These distributions should be proportional to a sum of $|Y_L^\lambda|^2$, where L is the spin and λ the helicity. We have fitted the distributions of Fig. 5b with a sum of three contributions, namely $|Y_0^0|^2$ (a constant), $|Y_2^2|^2$, and $|Y_2^0|^2$. We omit the $|Y_2^1|^2$ term because helicity 1 is not allowed for two real photons. We find that the $|Y_2^2|^2$-term dominates with a fraction of 0.81 ± 0.22. The spin-0 fraction is 0.19 ± 0.22 and the spin-2, helicity-0 fraction is 0 ± 0.08.[8] This agrees well with the expectation that for A_2, which has L = 2, the distribution will be proportional to a sum of $|Y_2^2|^2$ and $|Y_2^0|^2$. Furthermore, the helicity 2 term dominates the distribution as expected from theoretical predictions (see, e.g., Ref. 10) and previous measurements.[9,11] For the fit to Fig. 5a, we have used only the $|Y_0^0|^2$ and $|Y_2^2|^2$ terms. The $|Y_2^0|^2$ term was omitted because the previous fit showed that it was at most a small correction to the total spin-2 fraction. We find here the spin-0 fraction to be dominant (0.73 ± 0.29).

The $\Gamma_{\gamma\gamma}$-values resulting from the fit to Fig. 4 have been corrected by extrapolating to the full $\cos\Theta^*$ range assuming isotropy for the δ decay and helicity 2 for the A_2 decay. The known branching ratios[3] for $\eta \to \gamma\gamma$ and $A_2 \to \pi^0\eta$ have been taken into account. The

results are

$$\Gamma_{\gamma\gamma}(A_2) = (1.14 \pm 0.20 \pm 0.26)\,\mathrm{keV}$$

and

$$\Gamma_{\gamma\gamma}(\delta) \times \mathrm{BR}(\delta \to \pi\eta) = (0.19 \pm 0.07^{+0.10}_{-0.07})\,\mathrm{keV}.$$

The systematic errors include the following contributions added in quadrature:

- ▷ Uncertainty in the efficiency and $\gamma\gamma$ flux calculation ($\pm 10\%$)
- ▷ Uncertainty in the luminosity determination ($\pm 10\%$)
- ▷ Variation of analysis cuts (± 0.05 keV for δ, ± 0.14 keV for A_2)
- ▷ Variation of the fitting procedure ($^{+0.08}_{-0.04}$ keV for δ, ± 0.12 keV for A_2)
- ▷ Uncertainties of the branching ratios $\eta \to \gamma\gamma$ ($\pm 2\%$) and $A_2 \to \pi^0\eta$ ($\pm 8\%$) from Ref. 3

The δ has two known decay modes, $K\bar{K}$ and $\pi\eta$, with unknown branching ratios. In the literature quoted in Ref. 3, values for the $K\bar{K} : \pi\eta$ ratio are found varying between 1 : 4 and 4.2 : 1. If the coupling to $K\bar{K}$ is large, the resonance may have a width considerably larger than the observed peak width. The peak in this case would be generated as a cusp effect by the $K\bar{K}$ threshold[12]. The data do not allow us to distinguish this δ resonance shape from a simple Breit-Wigner shape. The result given is based upon a simple Breit-Wigner as described above.

$\Gamma_{\gamma\gamma}(\delta)$ (keV)	Authors
50	Bramón, Greco[13]
$2.5 - 3.8$	Berger, Feld[14]
$0 - 0.37$	Babcock, Rosner[10]
550 ± 270	Greenhut, Intemann[15]
4.8	Budnev, Kaloshin[16]
≈ 0.27	Achasov, Devyanin, Shestakov[17]

TABLE 1
Theoretical predictions for $\Gamma_{\gamma\gamma}(\delta)$.

The measured value of $\Gamma_{\gamma\gamma}(\delta) \times \mathrm{BR}(\delta \to \pi\eta)$ can be compared to the theoretical predictions of $\Gamma_{\gamma\gamma}(\delta)$ summarized in Table 1. If $\mathrm{BR}(\delta \to \pi\eta)$ is not small, only the predictions of Refs. 10 and 17 agree with our measurement, all others are at least an order of magnitude higher. Whereas Babcock and Rosner describe the δ as a $q\bar{q}$ state, it is a $q\bar{q}q\bar{q}$ state in the model of Achasov, Devyanin and Shestakov.

$\Gamma_{\gamma\gamma}(A_2)$ (keV)	Experiment
$0.77 \pm 0.18 \pm 0.27$	Crystal Ball at SPEAR[1]
$0.81 \pm 0.19 \pm 0.27$	CELLO[18]
$0.84 \pm 0.07 \pm 0.15$	JADE (preliminary)[11]
$1.06 \pm 0.18 \pm 0.19$	PLUTO[9]
$1.14 \pm 0.20 \pm 0.26$	This experiment

TABLE 2
Experimental results for $\Gamma_{\gamma\gamma}(A_2)$.

Our measurement of $\Gamma_{\gamma\gamma}(A_2)$ agrees within errors with previous measurements (Table 2). $\Gamma_{\gamma\gamma}(A_2)$ can also be predicted using quark model relations[19] and the measured value of $\Gamma_{\gamma\gamma}(f)$. The prediction is $\Gamma_{\gamma\gamma}(A_2) = 0.99 \pm 0.05\,\mathrm{keV}$[9], in good agreement with the measurements.

We would like to thank the DESY and SLAC directorates for their support. Special thanks go to the DORIS machine group and the experimental support groups at DESY. Some of us (A.F., Z.J., B.N., G.N. and T.S.) would like to thank DESY for financial support. A.F. in addition thanks the Deutsche Forschungsgemeinschaft and Hamburg University for financial support. D.W. acknowledges support from a National Science Foundation graduate fellowship. E.D.B., R.H. and K.S. have benefitted from Senior Scientists Awards from the Humboldt Foundation. The Nijmegen group acknowledges the support of FOM-ZWO. The Erlangen, Hamburg, and Würzburg groups acknowledge financial support from the Bundesministerium für Forschung und Technologie. This work was supported in part by the Department of Energy under contracts DE-AC03-81ER40050 (CIT), DE-AC02-76ER03066 (CMU), DE-AC02-76ER03064 (Harvard), DE-AC02-76ER03072 (Princeton), DE-AC03-76SF00515 (SLAC), and DE-AS03-76SF00326 (Stanford), and by the National Science Foundation under Grants PHY75-22980 (CIT), PHY84-07870 (HEPL), and PHY82-08761 (Princeton).

REFERENCES

1. Crystal Ball Collaboration, C. Edwards *et al.*, Phys. Lett. **110B** (1982), 82.

2. Crystal Ball Collaboration, M. Oreglia *et al.*, Phys. Rev. **D25** (1982), 2259;
   M. Oreglia, PhD thesis, Stanford U., SLAC-236 (1980), unpublished;
   J. Gaiser, PhD thesis, Stanford U., SLAC-255 (1982), unpublished.

3. Particle Data Group, *Review of Particle Properties*, Rev. Mod. Phys. **56** No.2, Part II (1984).

4. G. Bonneau, M. Gourdin and F. Martin, Nucl. Phys. **B54** (1973), 573.

5. R. Ford and W. Nelson, SLAC report 210 (1978).

6. $\sigma_{\gamma\gamma\to R\to\pi\eta}(W) = 8\pi(2L+1)\frac{\Gamma_{\gamma\gamma}(R)\,BR(R\to\pi\eta)\,\Gamma_R}{(m_R^2-W^2)^2+m_R^2\Gamma_R^2}$ with $R = \delta$ or A_2 and $L = 0$ or 2, respectively. We have used the following energy-dependent total width: $\Gamma_R(W) = \Gamma_R(m_R)(q/q_0)^{2L+1}\,D_L(q_0r)/D_L(qr)$, where q is the π momentum in the $\pi\eta$ rest frame and q_0 is the same calculated for $W = m_R$. D_L is the Blatt-Weisskopf barrier penetration function. The interaction length r is set to 1 fm[9].

7. The large error is caused by our mass resolution being comparable to the natural line width.

8. The sum of fractions was constrained to be equal to one in the fit, thus the errors are strongly correlated.

9. PLUTO Collaboration, Ch. Berger *et al.*, Phys. Lett. **149B** (1984), 427.

10. J. Babcock and J. L. Rosner, Phys. Rev. **D14** (1976), 1286.

11. J. E. Olsson (JADE Collaboration), in "Proc. 5th Int. Workshop on Photon-Photon Collisions (Aachen, 1983)", Springer Lecture Notes in Physics, Springer, Berlin, 1983, p. 45.

12. S. M. Flatté, Phys. Lett. **63B** (1976), 224;
    N. N. Achasov, S. A. Devyanin and G. N. Shestakov, Usp. Fiz. Nauk **142** (1984), 361;
    Sov. Phys. Usp. **27** (1984), 161.

13. A. Bramón and M. Greco, Lett. Nuovo Cimento **2** (1971), 522.

14. S. B. Berger and B. T. Feld, Phys. Rev. **D8** (1973), 3875.

15. G. K. Greenhut and G. W. Intemann, Phys. Rev. **D18** (1978), 231.

16. V. M. Budnev and A. E. Kaloshin, Phys. Lett. **86B** (1979), 351.

17. N. N. Achasov, S. A. Devyanin and G. N. Shestakov, Z. Phys. **C16** (1982), 55.

18. CELLO Collaboration, H. J. Behrend *et al.*, Phys. Lett. **114B** (1982), 378; *Erratum*, *ibid.* **125B** (1983), 518.

19. $\frac{\Gamma_{\gamma\gamma}(A_2)}{m^3_{A_2}} : \frac{\Gamma_{\gamma\gamma}(f)}{m^3_f} : \frac{\Gamma_{\gamma\gamma}(f')}{m^3_{f'}} = 3 : (\sin\vartheta + \sqrt{8}\cos\vartheta)^2 : (\sqrt{8}\sin\vartheta - \cos\vartheta)^2$, where ϑ is the singlet-octet mixing angle[9].

FIGURE CAPTIONS

1. (a) Scatterplot of $M^{high}_{\gamma\gamma}$ versus $M^{low}_{\gamma\gamma}$ (3 combinations per event) for events passing the two-photon selection criteria described in the text. (b) Same as (a), but $\pi^0\pi^0$ events removed.
2. p_T^2 distribution of $\pi^0\eta$ events (open histogram) and sideband events (shaded histogram, scaled by $\frac{1}{3}$, the ratio of areas in the mass scatter plot Fig. 1b).
3. W distribution of $\pi^0\eta$ events (open histogram) and sideband events (shaded histogram, scaled by $\frac{1}{3}$)
4. Cross section for $\gamma\gamma \to \pi^0\eta$ as function of W for $|\cos\Theta^*| < 0.9$. The solid curve is the result of a fit with $\delta(980)$, $A_2(1320)$ and non-resonant continuum contributions. The broken curve shows the continuum contribution.
5. Differential cross section $d\sigma/d|\cos\Theta^*|$ for (a) $900 < W < 1100\,\mathrm{MeV}$ and (b) $1100 < W < 1480\,\mathrm{MeV}$. Also shown are the fitted contributions proportional to $|Y^0_0|^2$ (dashed curve) and $|Y^2_2|^2$ (dotted curve) and their sum (solid curve).

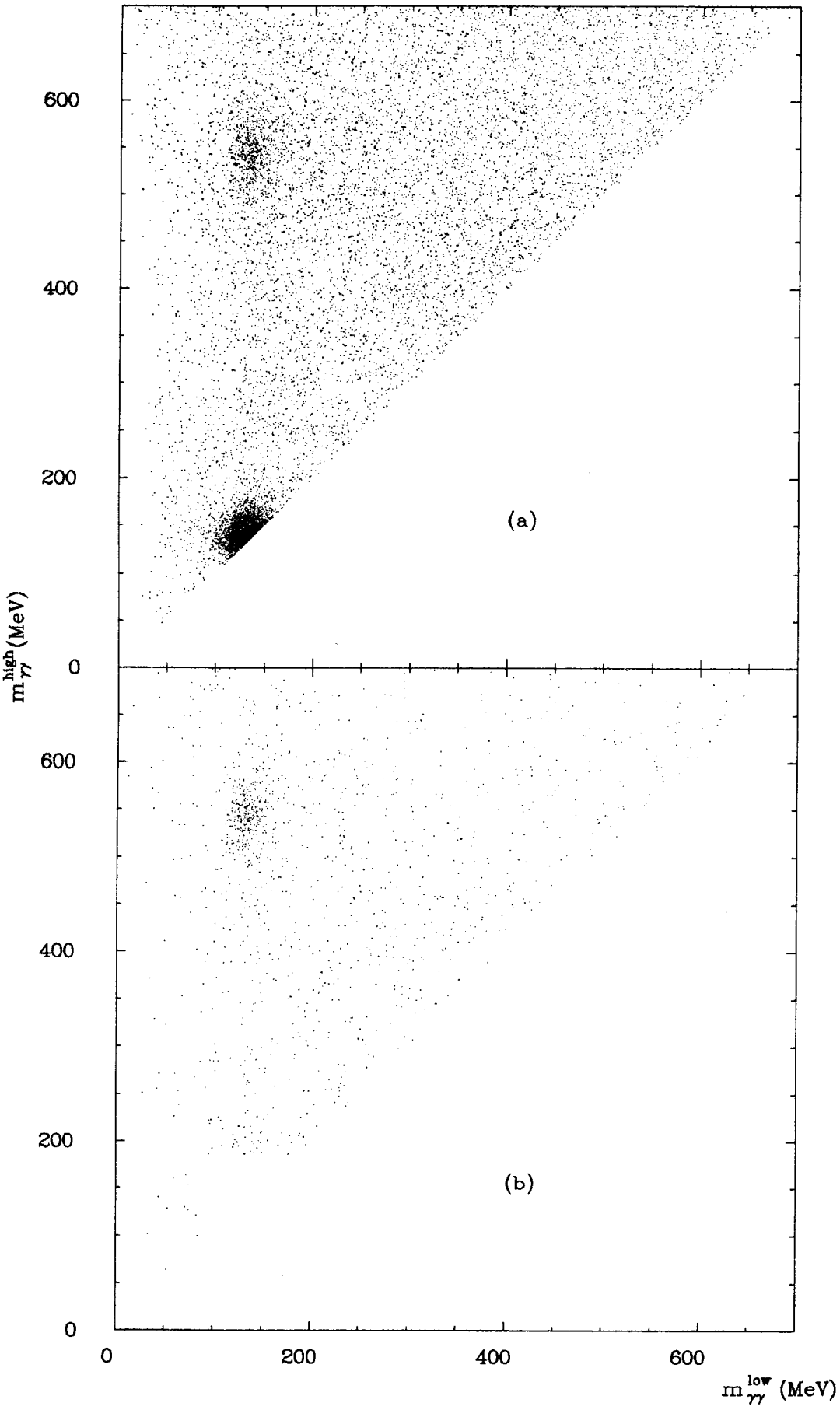
600
400
200
0
(a)
$m_{\gamma\gamma}^{high}$ (MeV)
600
400
200
0
(b)
0
200
400
600
$m_{\gamma\gamma}^{low}$ (MeV)

Fig. 1

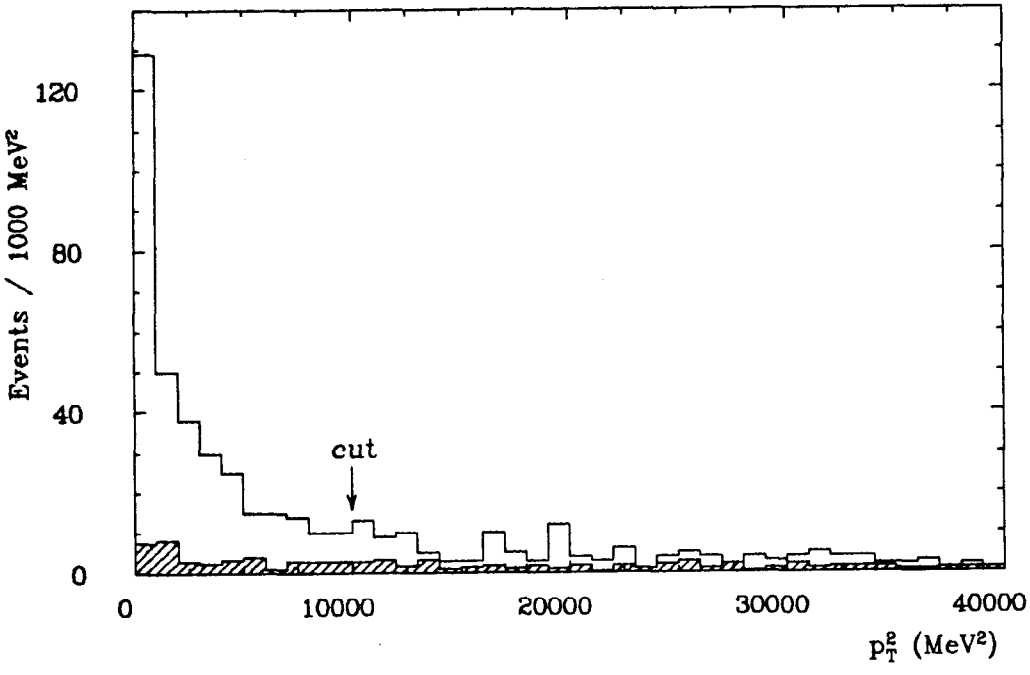
120
80
40
0
Events / 1000 MeV²
cut
0
10000
20000
30000
40000
p_T^2 (MeV²)

Fig. 2

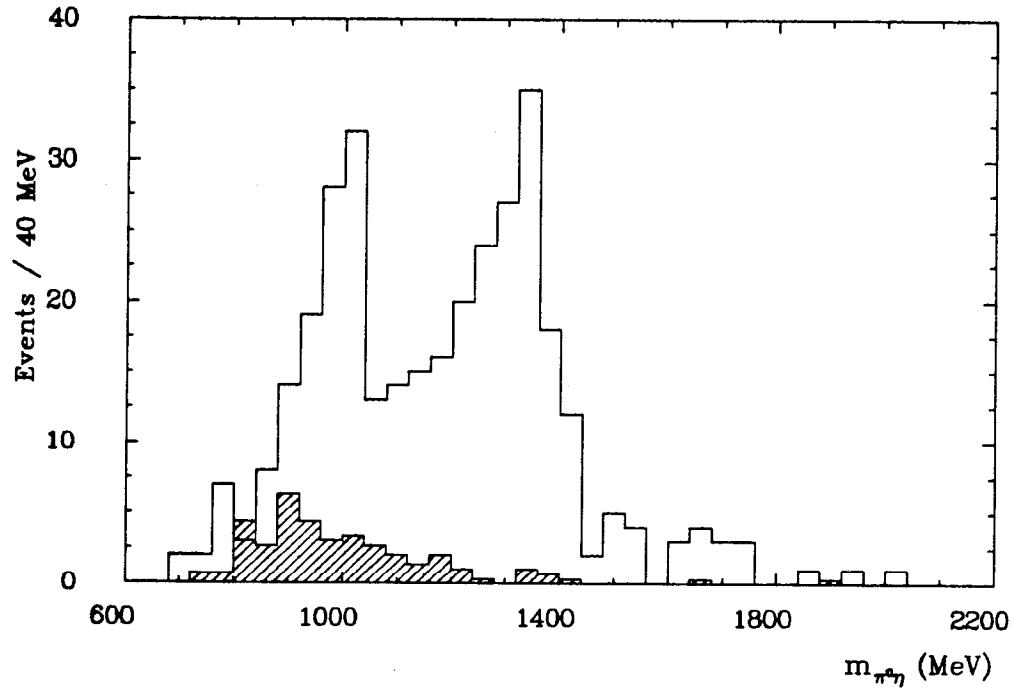

Fig. 3

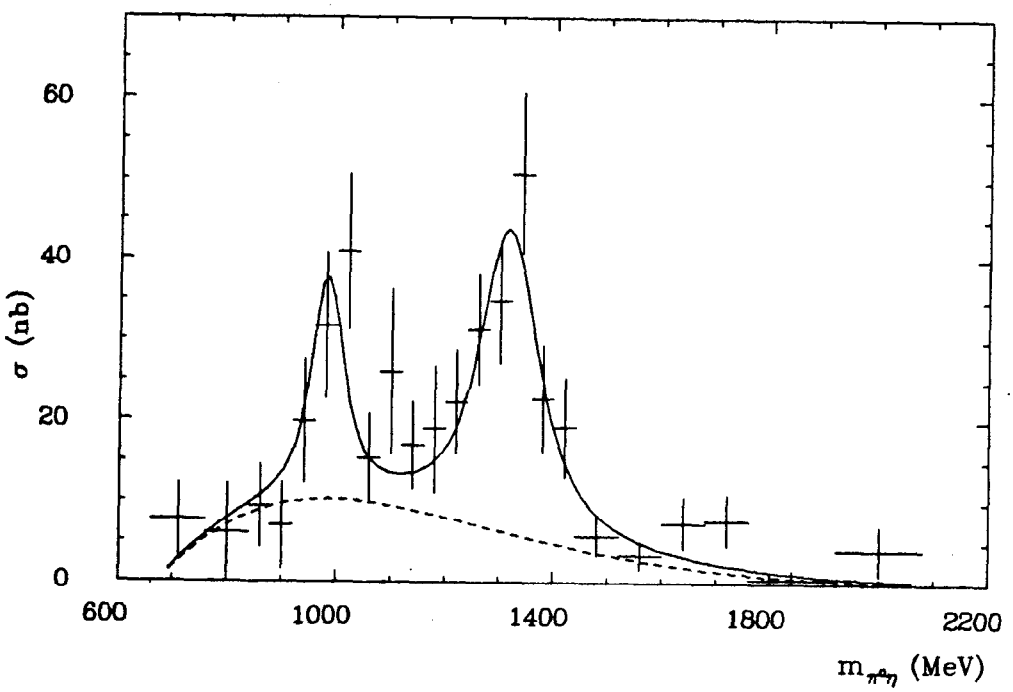

Fig. 4

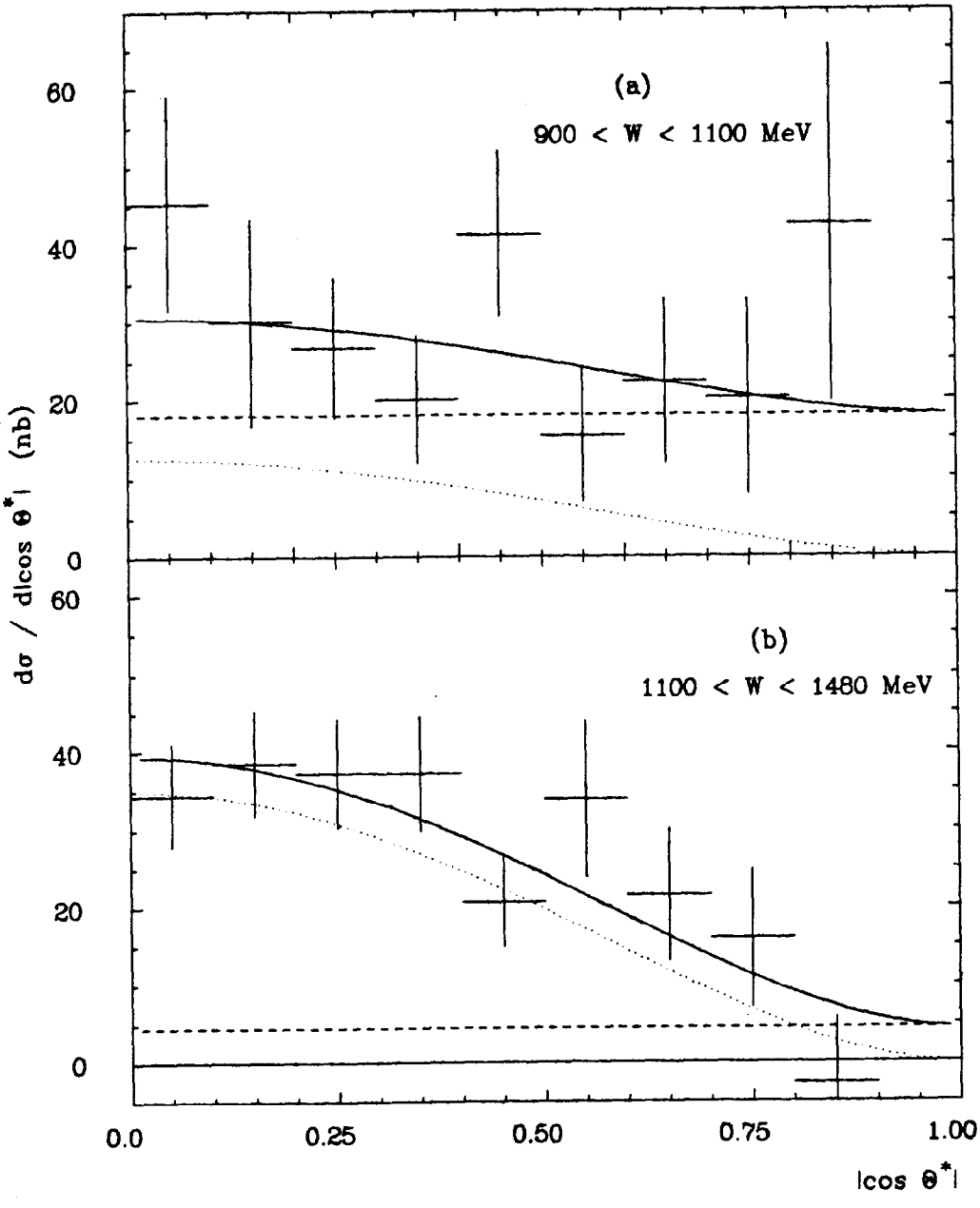
(a)
900 < W < 1100 MeV
(b)
1100 < W < 1480 MeV
dσ / dlcos θ*l (nb)
60
40
20
0
60
40
20
0
0.0
0.25
0.50
0.75
1.00
lcos θ*l

Fig. 5